

Discovery of polarizations from ground state absorption lines: tracer of sub-Gauss magnetic field on 89Her

HESHOU ZHANG,^{1,2} MANUELE GANGI,^{3,4} FRANCESCO LEONE,⁵ ANDREW TAYLOR,¹ AND HUIRONG YAN^{1,2}

¹Deutsches Elektronen-Synchrotron DESY, Platanenallee 6, D-15738 Zeuthen, Germany

²Institut für Physik und Astronomie, Universität Potsdam, Haus 28, Karl-Liebknecht-Str. 24/25, D-14476 Potsdam, Germany

³INAF - Osservatorio Astrofisico di Catania, Via S. Sofia 78, I-95123 Catania, Italy

⁴INAF - Osservatorio Astronomico di Roma, Via Frascati 33, I-00078 Monte Porzio Catone, Italy

⁵Università di Catania, Dipartimento di Fisica e Astronomia, Sezione Astrofisica, Via S. Sofia 78, I-95123 Catania, Italy

ABSTRACT

We report the identification of the polarization of ground state absorption lines from post-AGB 89 Hercules. Two ground state neutral iron lines are found to have counterintuitive high-amplitude polarizations and an unchanged polarization direction through the orbital period, as opposed to the pattern of polarizations of absorption lines from excited states, which are synchronized with the orbital phase owing to optical pumping. This can be explained with magnetic realignment on the ground state. The 3D mean magnetic field is thereby unveiled from the degree and direction of the polarizations of the two iron lines. The field strength is also constrained to be $\lesssim 100$ mG. Our result has thus improved the accuracy by orders of magnitude compared to the previous 10 G upper limit set by non-detection of the Zeeman effect.

1. INTRODUCTION

Spectral polarimetry observations can provide exclusive information on magnetic field and topology of the radiation structure. Developments on high-resolution spectral facilities with polarimeters (e.g., PEPsi, Strassmeier et al. 2008; HARPS, Piskunov et al. 2011; HANPO, Leone et al. 2014) allows the investigation of polarimetric properties of single spectral lines. The surprisingly high polarimetric signals shown by the prototypical star 89 Herculis (in average, more than 1%) give us the unique opportunity to study this system (Leone et al. 2018).

89 Herculis (89 *Her*) is a post-AGB binary system. The primary star is an F-type supergiant with a radius $R_{pri} = 41R_{\odot}$ and an effective temperature $T_{eff} = 6500K$ while the secondary is an M-type main sequence with $R_{sec} = 0.6R_{\odot}$ and $T_{eff} = 4045K$. The radius of the secondary orbital track is $r_{orb} = 67R_{\odot}$. 89 *Her* has an orbital period $P_{orb} \sim 288$ days and inclination 12° . It presents a circumstellar environment consisting of two main components: an expanding hour-glass structure and an circumbinary rotating disk (Waters et al. 1993; Kipper 2011a; Bujarrabal et al. 2007). The projection of stellar outflows on the picture plane is 45° comparing to the East-West orientation (Bujarrabal et al. 2007). Leone et al. (2018) has found that linearly polarized photospheric absorption lines of 89 Her present Q/I and U/I sig-

nals varying according to the secondary orbital period (hereafter “orbital synchronization”). They have excluded the origin of such signal from either the depolarization of stellar continuum polarization (incl. pulsations, hot spots), or scattered polarization from a bipolar outflows, and found that it is a result of the optical pumping in the stellar environment.

In this letter, we report the discovery of two ground state Fe I photosphere absorption line polarizations, whose directions have not shown “orbital synchronization”, but rather are aligned through all orbital phases¹. This observation indicates the existence of ground state magnetic alignment, which was first theoretically proposed as a magnetic tracer in (Yan & Lazarian 2006). The alignment is in terms of the angular momentum of atoms and ions (hereafter “atoms” for simplicity). The ground state alignment (henceforth GSA) is an established physical phenomenon which has solid physical foundations and has been studied and supported by numerous experiments (Kastler 1950; Brossel, Jean et al. 1952; Hawkins & Dicke 1953; Hawkins 1955; Cohen-Tannoudji et al. 1969). The anisotropic radiation aligns the atoms on the ground state by optical pumping (Happer 1972; Varshalovich 1971; Landolfi & Landi Degl’Innocenti 1986). These radiative aligned atoms are magnetically realigned by fast precession as long as the Larmor precession rate ν_{Lar} is larger than the radiative pumping rate ν_{Rad} (Yan & Lazarian 2006, 2007). In the GSA regime, the atoms are aligned with radi-

Corresponding author: Huirong Yan
huirong.yan@desy.de

¹ Hereafter, we will assume the same ephemeris adopted in (Leone et al. 2018) to compute the orbital phases of 89 Her (*iph*).

ation field or realigned by magnetic field depending on the ratio of the two rates ($r_A \equiv \nu_{\text{Lar}}/\nu_{\text{Rad}}$). In the Ground level Hanle regime, however, the atoms preferentially follow neither the magnetic or radiation field ($r_A \sim 1$) (Yan & Lazarian 2008). The GSA probe is particularly suitable for sub-Gauss magnetic field since the atoms have long life time in their ground states. The resulting absorption lines from the aligned atoms are polarized parallel or perpendicular to the magnetic field direction.

The magnetic field in the 89Her’s primary has been unknown. Earlier attempts with current magnetic tracers have not provided strong constraint: no continuum polarization is detected (see Akras et al. 2017) and previous spectropolarimetric studies have revealed that the source is circularly unpolarized, which only implies an upper limit of 10 G (Sabin et al. 2015). In the letter, we will first discuss the observational results and then provide the theoretical interpretations, which lead to the extraction of the mean magnetic field information on the photosphere of the 89 Her’s primary.

2. OBSERVATIONAL DATA

Reduced spectropolarimetric data of 89 Her have been collected at the 3.6-m Canada-France-Hawaii Telescope with the Echelle SpectroPolarimetric Device for the Observation of Stars (ESPaDOoS: R=68000, Donati et al. 2006). They consist of Stokes I , Q , U , and *null* NQ , NU (Leone et al. 2016). From these data we computed the polarization P , the *null* polarization NP and the polarization angle ξ , according to the definitions given in Landi Degl’Innocenti & Landolfi (2004). The spectral lines studied are unblended with other lines, as shown in Fig. 1(a-c)². To provide an objective criterion for deciding whether a polarimetric signal is detected across the spectral lines, we follow the statistical test of Donati et al. (1997). Firstly we computed the reduced χ^2 inside and outside the spectral lines for both P and *null* NP profiles. Then we calculated the χ^2 detection probabilities based on the achieved signal-to-noise ratio (S/N), as shown in Table 1 in Supplementary. We concentrate on the central part of the absorption line (corresponding to the marked green zone in Fig. 2d), which is least influenced by the blue and red shifted emission from outflows.

3. POLARIZATION ANALYSIS FOR THE PHOTOSPHERIC ABSORPTION LINES

Previous spectropolarimetric works focus only on lines with a relatively large optical depth ($\tau \gtrsim 0.5$). We found that all the photosphere lines showing “orbital synchronization”

stand for the transitions between the excited states. As an example, the linear polarization profile of Fe II $\lambda 5362.970 \text{ \AA}$ ($10.50\text{eV} \rightarrow 12.81\text{eV}$) is presented in Fig. 1d, showing the correlation between their polarization angle and the vector connecting the two stellar bodies during their orbits (see Fig. 2a).

Here we focus on two ground state neutral iron absorption lines, Fe I $\lambda 5060.249 \text{ \AA}$ ($0\text{eV} \rightarrow 2.45\text{eV}$) and Fe I $\lambda 5166.282 \text{ \AA}$ ($0\text{eV} \rightarrow 2.40\text{eV}$). These lines are weak ($\tau \sim 0.2$, see Fig. 1b,c) and therefore were previously ignored. As demonstrated in Fig. 1(e,f), they have shown counterintuitive strong polarization signatures. Moreover, the polarization angles of these two Fe I lines are aligned through all orbital phases (see Fig. 2b) towards $\sim 45^\circ$ to East-West orientation. Such results indicate that the atomic angular momentum on the ground state is realigned by fast magnetic precession, in other words, the magnetic realignment dominates over optical pumping. We note that at $iph = 0.325$, the polarization direction of the radiation dominant lines are the same as that of GSA lines. This is because the radiative pumping direction at this phase coincides with the magnetic alignment direction.

We find that only the absorption term of linear polarization is important to account for in the analysis of these two GSA lines. The reasons are the following: (1) The background stellar continuum is unpolarized (Akras et al. 2017); (2) The spontaneous (scattered) emission from “the upper states” are negligible (see Fig. 3a for microphysics). The upper states of those two transitions have different angular momentum ($J_u = 3, 5$ respectively). Hence the scattered emission would yield a different polarization profile between the two lines at different iph . This is at odds with the observations of the aligned polarization direction. (3) The polarization signals for absorption from “the upper states” also support our conclusion (see Fig. 3b). We consider the absorption line Fe I $\lambda 4187.039 \text{ \AA}$ ($2.45\text{eV} \rightarrow 5.41\text{eV}$), i.e., the absorption from “the upper level” 2.45eV . Its Stokes Q and U signals are compared with two types of lines: “the pumping dominant reference” Fe II $\lambda 5362.970 \text{ \AA}$ and the GSA line Fe I $\lambda 5060.249 \text{ \AA}$. The orbital variation pattern of Fe I $\lambda 4187.039 \text{ \AA}$ ($2.45\text{eV} \rightarrow 5.41\text{eV}$) is similar to the Fe II $\lambda 5362.970 \text{ \AA}$ line, showing a varying radiative alignment of atoms on 2.45eV . This level’s varying contribution to the unchanged polarization signal of the ground state absorption line Fe II $\lambda 5060.249 \text{ \AA}$ is therefore negligible. Magnetic alignment happens only on the ground state.

4. THEORETICAL ANALYSES

4.1. Theoretical expectations and the identification of the 2D magnetic field

We solve the atomic transition equations to estimate the expected level of polarization signals from 89 Her (see App.

² Unlike Na D lines and Balmer lines in 89 Her, where the photospheric line is blended with multiple blue-shifted absorption components as well as redshifted strong interstellar absorption (see, e.g., Kipper 2011b; Gangi & Leone 2019).

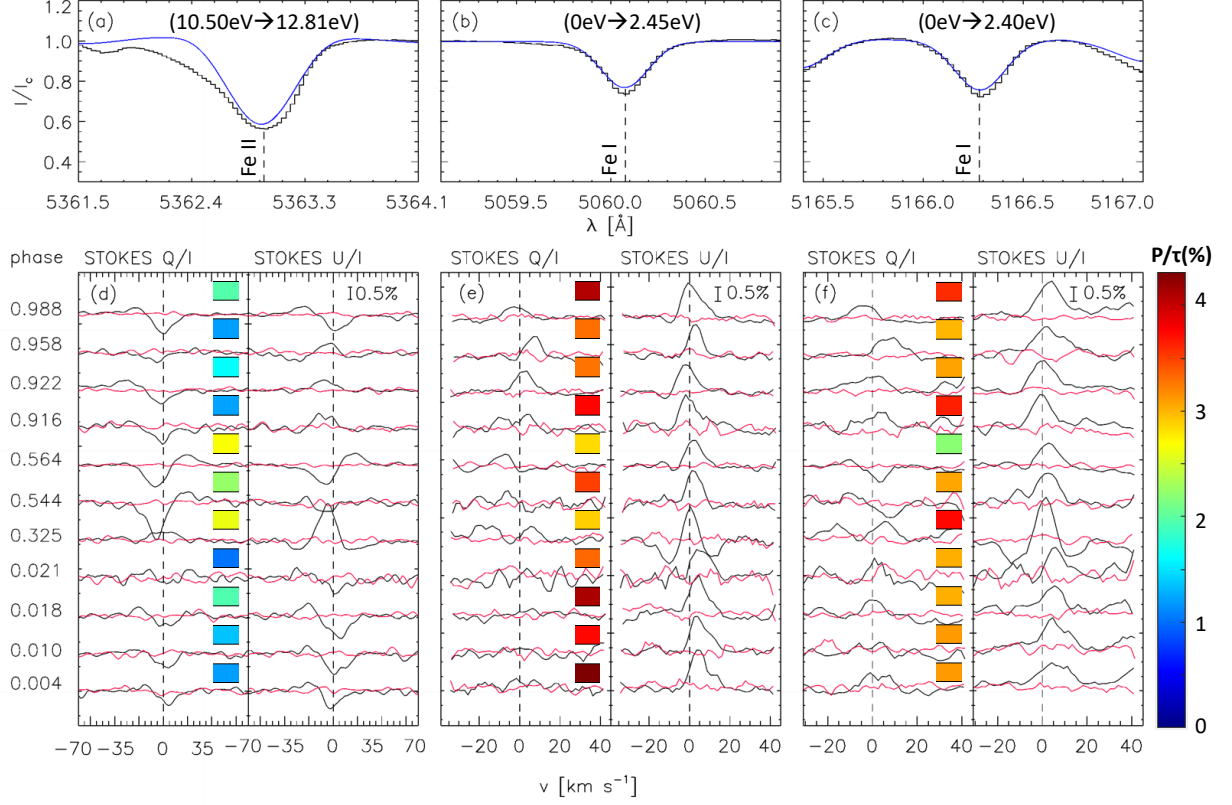


Figure 1. *Upper:* (a) The observed spectral line profile (black) and its comparison with the photospheric lines modeled (blue) with the synthetic spectrum package SYNTHE (Kurucz 2005) for the radiative dominant line Fe II $\lambda 5362.970$ Å (a), and of the two magnetic aligned lines Fe I $\lambda 5060.249$ Å (b) and Fe I $\lambda 5166.282$ Å (c). These lines are unblended and identified from photosphere. *Middle:* Q/I and U/I profiles of (d) Fe II $\lambda 5362.970$ Å, (e) Fe I $\lambda 5060.249$ Å, (f) Fe I $\lambda 5166.282$ Å lines. The *null* spectra are marked with red color. The degree of polarization P in each phase is denoted by the color mark.

B for details). The ground state is taken to be fully magnetically aligned and the anisotropic pumping is provided by the secondary. The 90° –ambiguity (known as Van Vleck ambiguity, Van Vleck 1925; House 1974) between the observed polarization and the position of sky (henceforth POS) magnetic projection is also resolved from the comparison of theoretical expectations and the observed degree of polarization. We scan the full parameter space to solve the expected maximum alignment parameter and the ratio of polarization P/τ . Given the face-on orbit, we take the radiation from the secondary in the range $\theta_0 \in [65^\circ, 90^\circ]$. We find that in the case of parallel alignment ($\varepsilon_\sigma = +1$), the expected maximum polarization signal can reach $P_{\max}/\tau(5060\text{Å}) \gtrsim 8\%$, $P_{\max}/\tau(5166\text{Å}) \gtrsim 4\%$, respectively. These upper limits for the two lines are consistent with the observed polarization signals of both the ground state absorption lines. Nonetheless, the maximum P_{\max}/τ in the case of perpendicular alignment ($\varepsilon_\sigma = -1$) calculated from the transitional equation are 4.9% and 2.5% for the two absorption lines $\lambda 5060.249$ Å, $\lambda 5166.249$ Å, respectively, smaller than

the observed values. The perpendicular alignment is thus excluded.

4.2. Magnetic field in the 3rd dimension

The theoretical Stokes parameters $[\tilde{I}, \tilde{Q}, \tilde{U}, \tilde{V}]$ are defined with \tilde{Q} measured from the magnetic field direction on the plane of sky (see x_0y_0z –frame Fig. 2c). In the case of purely absorbing medium, they are given by Yan & Lazarian (2006):

$$\begin{aligned}\tilde{I} &= (I_0 + Q_0)e^{-\tau(1+\eta_1/\eta_0)} + (I_0 - Q_0)e^{-\tau(1-\eta_1/\eta_0)}, \\ \tilde{Q} &= (I_0 + Q_0)e^{-\tau(1+\eta_1/\eta_0)} - (I_0 - Q_0)e^{-\tau(1-\eta_1/\eta_0)}, \\ \tilde{U} &= U_0e^{-\tau}, \tilde{V} = V_0e^{-\tau},\end{aligned}\tag{1}$$

where η_i are absorption coefficients of the Stokes parameters. Theoretically, the absorption coefficients are determined by (see Landi Degl’Innocenti 1984):

$$\begin{aligned}\eta_i(\nu, \Omega) &= \frac{h\nu_0}{4\pi} Bn(J_l)\xi(\nu - \nu_0) \sum_{kq} (-1)^k \\ &\times w_{J_l J_u}^{(k)} \sigma_q^k(J_l) \mathcal{J}_q^k(i, \Omega).\end{aligned}\tag{2}$$

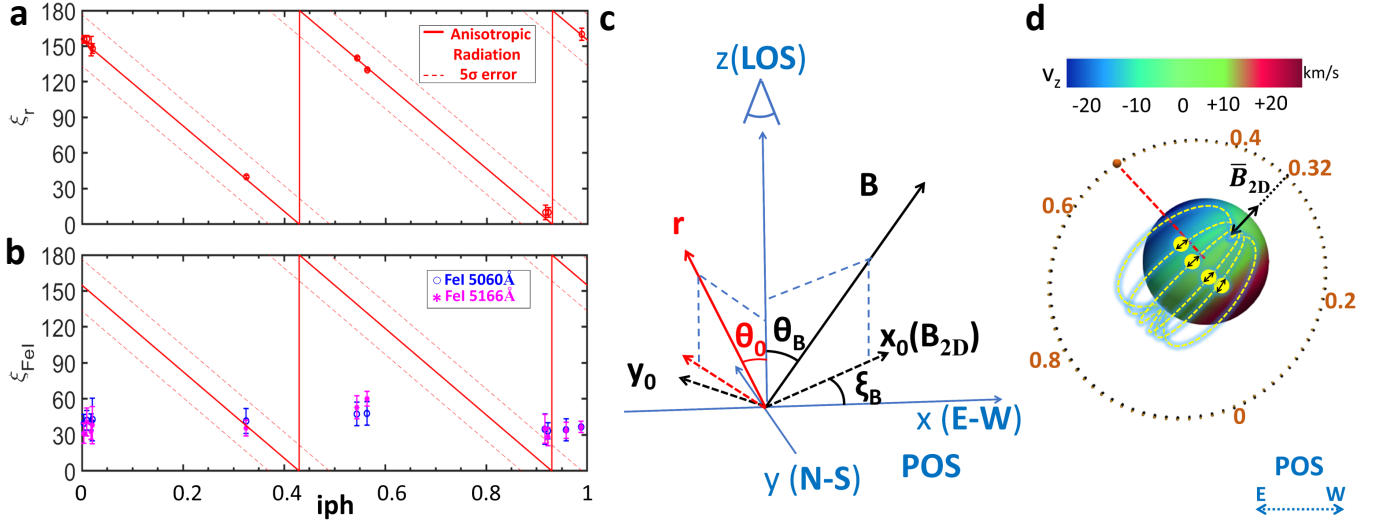


Figure 2. (a) strong absorption lines between excited states, the polarization angle (ξ_r) shows “orbital synchronization”. iph is orbital phase; (b) the polarization angle ξ_{FeI} for the two Fe I lines. The error bars mark the 3σ uncertainty range. (c) 3D view of the system showing the reference frame. xyz -frame is the observational frame where ox -axis is defined arbitrarily on East-West direction. θ_B and ξ_B are the polar and azimuth angles for magnetic field in the frame. x_0y_0z -frame is the theoretical frame where ox_0 -axis is the direction of the plane-of-sky magnetic field projection. (d) 89 *Her* system. The orbital phases are marked along the secondary track. The color scale denotes the line-of-sight (henceforth LOS) velocity (v_z) of the photosphere medium. Our analysis measures the mean magnetic field in the green region of the primary’s photosphere, corresponding to the central part of the absorption lines. A possible magnetic tomography of the system is presented here. The yellow dashed lines are magnetic field lines. The double arrows are the polarization directions. The average magnetic field projection on POS \bar{B}_{2D} is $\sim 45^\circ$ to the East-West direction pointing to the orbital phase 0.32.

where $\sigma_q^k(J_l) \equiv \rho_q^k(J_l)/\rho_0^0(J_l)$, $\rho_q^k(J_l)$ is the irreducible density matrix on the ground state. In the GSA regime, only $q = 0$ is non-zero and $\sigma_0^2(J_l)$ is the alignment parameter (Yan & Lazarian 2006). The quantity $n(J_l)$ is the population on the lower level. The quantity $\mathcal{J}_q^k(i, \Omega)$ is the irreducible unit tensors for Stokes parameters I, Q, and U. The ratio η_1/η_0 in the GSA regime is then (Yan & Lazarian 2006):

$$\eta_1/\eta_0 = -\frac{1.5\sigma_0^2(J_l)\sin^2\theta_B w_{J_l J_u}^{(2)}}{\sqrt{2} + \sigma_0^2(J_l)(1 - 1.5\sin^2\theta_B)w_{J_l J_u}^{(2)}}, \quad (3)$$

where θ_B is the angle between magnetic field and the line of sight.

$$w_{J_l J_u}^{(2)} \equiv \left\{ \begin{array}{ccc} 1 & 1 & 2 \\ J_l & J_l & J_u \end{array} \right\} / \left\{ \begin{array}{ccc} 1 & 1 & 0 \\ J_l & J_l & J_u \end{array} \right\},$$

is determined by the electron configurations of the transition $J_l \rightarrow J_u$. The alignment parameter σ_0^2 is the same for two transitions with the same ground level ($J_l \rightarrow J_{u1}$, $J_l \rightarrow J_{u2}$). Different observed degree of polarization for these two lines results from the angular momentum configuration parameters $w_{J_l J_{u1}}^{(2)}, w_{J_l J_{u2}}^{(2)}$. Therefore, we obtained

from Eq.(3):

$$\sigma_0^2(J_l) = \begin{cases} \frac{\sqrt{2}(c_1 c_2 (w_{J_l J_{u2}}^{(2)} - w_{J_l J_{u1}}^{(2)}) + \varepsilon_\sigma (c_1 w_{J_l J_{u2}}^{(2)} - c_2 w_{J_l J_{u1}}^{(2)}))}{(c_2 - c_1) w_{J_l J_{u1}}^{(2)} w_{J_l J_{u2}}^{(2)}}, \\ \text{sgn}(w_{J_l J_{u1}}^{(2)}) = \text{sgn}(w_{J_l J_{u2}}^{(2)}); \\ -\frac{\sqrt{2}(c_1 c_2 (w_{J_l J_{u2}}^{(2)} - w_{J_l J_{u1}}^{(2)}) + \varepsilon_\sigma (c_1 w_{J_l J_{u2}}^{(2)} + c_2 w_{J_l J_{u1}}^{(2)}))}{(c_1 + c_2) w_{J_l J_{u1}}^{(2)} w_{J_l J_{u2}}^{(2)}}, \\ \text{sgn}(w_{J_l J_{u1}}^{(2)}) = -1, \text{sgn}(w_{J_l J_{u2}}^{(2)}) = +1; \end{cases}$$

$$\sigma_0^2(J_l) \sin^2\theta_B = \begin{cases} \frac{2\sqrt{2}c_1 c_2 (w_{J_l J_{u2}}^{(2)} - w_{J_l J_{u1}}^{(2)})}{3(c_2 - c_1) w_{J_l J_{u1}}^{(2)} w_{J_l J_{u2}}^{(2)}}, \\ \text{sgn}(w_{J_l J_{u1}}^{(2)}) = \text{sgn}(w_{J_l J_{u2}}^{(2)}); \\ -\frac{2c_1 c_2 (w_{J_l J_{u2}}^{(2)} - w_{J_l J_{u1}}^{(2)})}{3(c_1 + c_2) w_{J_l J_{u1}}^{(2)} w_{J_l J_{u2}}^{(2)}}, \\ \text{sgn}(w_{J_l J_{u1}}^{(2)}) = -1, \text{sgn}(w_{J_l J_{u2}}^{(2)}) = +1; \end{cases} \quad (4)$$

The ratio $c_j \equiv |\eta_1/\eta_0| = \frac{1}{2\tau_j} \ln\left(\frac{1+P_j}{1-P_j}\right)$, $j = 1, 2$ is directly related to the degrees of polarization and optical depths of a doublet (see Eq. 1). The quantity ε_σ is the sign of the alignment parameter for the lower level $\sigma_0^2(J_l)$. The positive alignment $\varepsilon_\sigma = +1$ corresponds to the alignment of the angular momentum on ground states being parallel to the magnetic field, whereas the negative alignment $\varepsilon_\sigma = -1$ means it is perpendicular. The averaged magnetic field po-

lar angle in the absorbing volume can hence be achieved by $\sin^2 \theta_B = \int dV_{abs} \sigma_0^2(J_l) \sin^2 \theta_B / \int dV_{abs} \sigma_0^2(J_l)$.

In the case of the two Fe I absorption lines, the configuration parameters of these two transitions are of the same sign: $w_{J_l J_{u1}}^{(2)} = \omega_{4,3}^{(2)} = 0.4432$; $w_{J_l J_{u2}}^{(2)} = \omega_{4,5}^{(2)} = 0.2256$. Therefore, the corresponding results are:

$$\sigma_0^2(J_l) = \frac{-0.2176c_1c_2 + \varepsilon_\sigma(0.2256c_1 - 0.4432c_2)}{0.0707(c_2 - c_1)}, \quad (5)$$

The alignment is parallel, i.e., $\varepsilon_\sigma = 1$. θ_B can then be also obtained by solving the Eq.(5). The resulting θ_B, ξ_B and their error bars in different phases are presented in Table 1 (see Fig. 2c for 3D geometry). As illustrated in Fig. 2d, a dipole magnetic field on the stellar surface can support such analysis reasonably, with the average 2D magnetic field parallel to the outflow orientation on POS.

Table 1. 3D magnetic field angles. The POS component ξ_B and LOS component θ_B as demonstrated in Fig. 2c. $\Delta\xi_B$ is the 3σ error bar obtained from the observed direction of polarization and $\Delta\theta_B$ is the 1σ error bar inferred from the degree of the polarization (§4.1).

iph	ξ_B	$\Delta\xi_B$	θ_B	$\Delta\theta_B$
0.004	35.5	7.9	62.4	11.0
0.01	41.5	10.0	56.8	15.9
0.018	36.8	6.6	58.6	13.6
0.021	40.5	16.6	54.9	14.6
0.325	38.7	8.5	55.6	11.9
0.544	50.2	9.7	59.3	11.1
0.564	54.0	8.0	53.2	11.0
0.916	35.0	12.3	57.0	15.6
0.922	30.9	7.2	54.5	13.8
0.958	34.1	8.1	56.0	14.3
0.988	36.7	4.7	67.6	8.3

4.3. Constraining the magnetic field strength

Magnetic field strength of 89 *Her* is not directly available since both the radiative alignment on the upper states and the magnetic realignment are saturated effects. Nonetheless, the magnetic field strength can be constrained by comparing the life time of different states (either radiative pumping rate or spontaneous emission rate) with the Larmor precession rate ($\omega_{Lar} \sim 17.6(\text{B}/\mu\text{G})$). On one hand, the radiative pumping rate from the Fe I ground state³ is much smaller than the

Larmor precession rate, $\max\{\nu_{Rad}\} < 0.1\nu_{Lar}$. With the secondary providing the optical pumping, the magnetic field strength lower limit is $\sim 10\mu\text{G}$ (see Fig. 4).

On the other hand, the synchronization between pumping direction and polarizations of lines from the excited states shows that the escaping rate from the excited states, which includes both radiative pumping and spontaneous emission, dominates over the Larmor precession rate on the excited states. Hence the upper limit of the magnetic field strength can be narrowed by $10\nu_{Lar} < \max\{\nu_{Rad}, \nu_{Em}\}$. Utilizing the fact that Fe II $\lambda 5362.970 \text{ \AA}$ ($10.50\text{eV} \rightarrow 12.81\text{eV}$) absorption line is fully radiative aligned for all the orbital phases, we deduce the upper limit field strength being $\sim 108m\text{G}$. Additionally, we find that the Fe I $\lambda 5586 \text{ \AA}$ ($3.37\text{eV} \rightarrow 5.59\text{eV}$) absorption line presents a more than 3σ detectability polarization signal at the orbital phases 0.544, 0.564, 0.988 and that the polarization direction for all those phases aligns with radiative pumping direction rather than magnetic field direction. This gives us an upper limit for the field strength of $\sim 80m\text{G}$. The accuracy of the field strength is increased by at least two decades compared to the previous 10 G upper limit, constrained from the non-detection of the Zeeman effect.

5. DISCUSSION

GSA is the most probable and natural explanation for the discovered polarization signals of the ground state absorption lines, that are realigned to one direction as opposed to the “orbital synchronization”. We provide here the mean magnetic field of the photosphere surface medium that corresponds to the central part of the absorption line. Fig. 2d serves illustratively that such magnetic field is reasonable on the stellar surface. A full magnetic field tomography requires further studies, which is beyond the scope of current observation precision. Higher resolution spectral observation will enable us to study the wings in the absorption line profiles, separating the emission components from outflows.

Through our analyses, we assume the anisotropic pumping comes from the secondary (following Leone et al. 2018). However, when constraining the magnetic field strength, a narrower range might be achieved if accounting for the photons from the primary. We calculate the extended radiation field of the primary following (Zhang et al. 2015) with the Lambert cosine law and limb-darkening (Claret & Bloemen 2011) considered, and find that the lower limit for magnetic field strength can be $\sim 2m\text{G}$ (see Fig. 4a). Additionally, we could interpret the “orbital synchronization” as a result of local polarized flux illuminating the medium rather than pumping from the secondary. Nonetheless, even under such assumption, the realigned polarization direction of two ground state lines we report here can still be explained by the mag-

³ All transitions from the given level are taken into account (both excitations and spontaneous emission) when the escaping rate from a level is calculated. The NIST Atomic Spectra Database is adopted for the Einstein coefficients to calculate the pumping rate. A total of 47 transitions from Fe I ground state and 38 transitions from the state Fe II (10.50eV) are included.

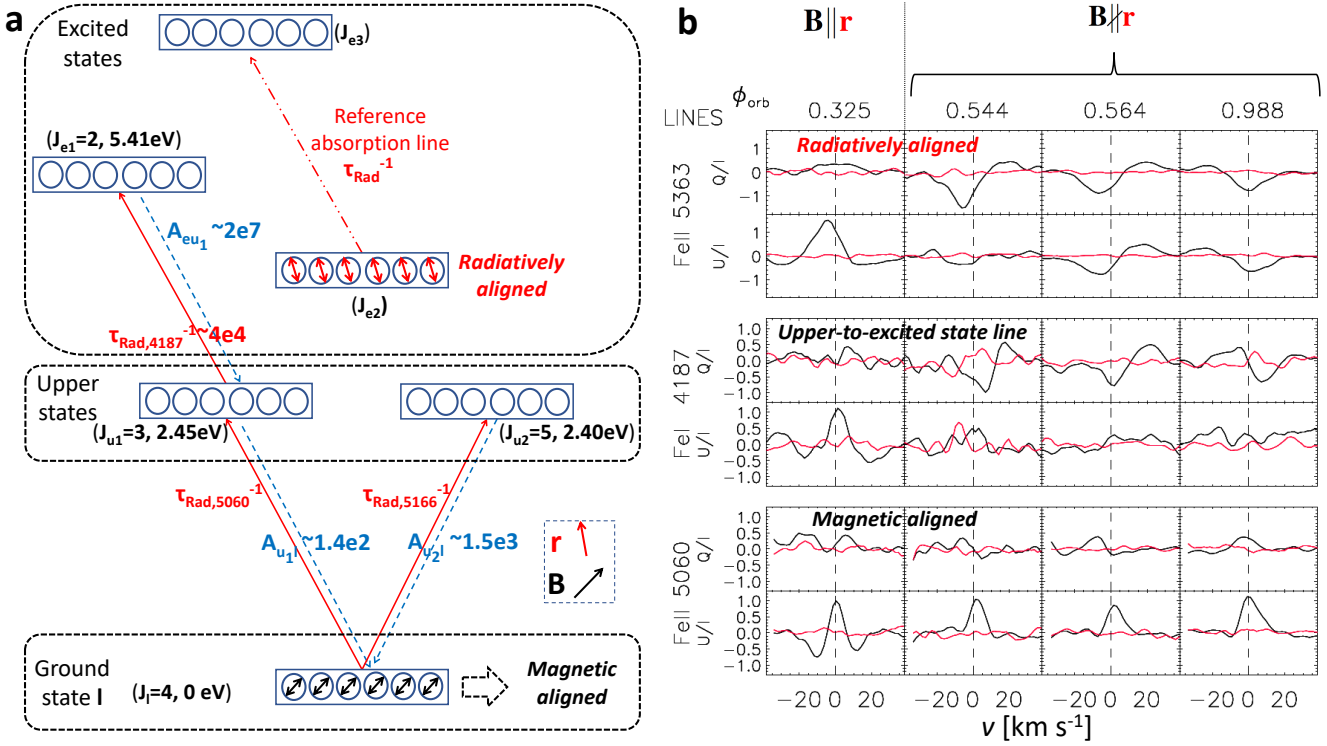


Figure 3. (a) Schematics of the optical pumping and magnetic realignment in the GSA regime. Rectangles with circles represent the energy state occupied by atoms. The arrows are the atomic angular momentum. The ground state is magnetically aligned. “The upper states” mark the upper levels for transitions of focus Fe I $\lambda\lambda 5060, 5166 \text{ \AA}$. Other states are marked as excited states. The Einstein coefficients for transitions involving the level Fe I 2.45 eV are marked. (b) Stokes parameters of the selected absorption lines. They are: the pumping reference Fe II $\lambda 5362.970 \text{ \AA}$; Fe I $\lambda 4187.039 \text{ \AA}$ from “the upper state” 2.45 eV ; the GSA line Fe I $\lambda 5060.249 \text{ \AA}$ at 4 different orbital phases: 0.325, 0.544, 0.564, 0.988.

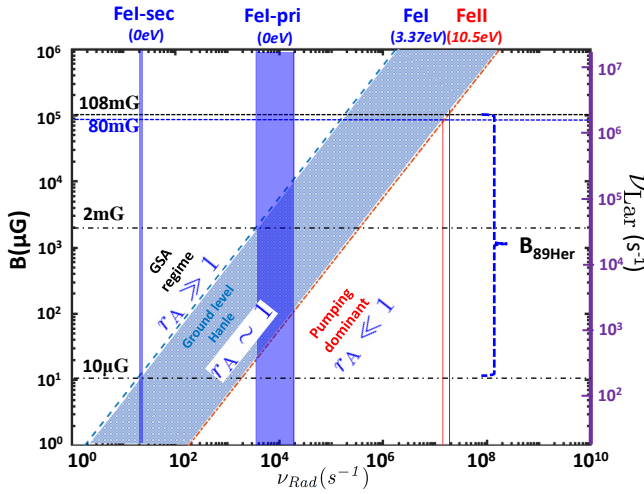


Figure 4. Magnetic field strength in 89 Her. The escaping rates from Fe I (0 eV), and from Fe I (3.37 eV), Fe II (10.5 eV), are marked on top. The dash-dotted lines mark the lower limits of magnetic field strength, estimated based on the assumption of optical pumping by the secondary and primary, respectively. The dashed lines show the upper limit of magnetic field strength derived from different transitions.

netic realignment of the angular momentum on the ground state.

Moreover, beyond optical band, GSA can be implemented with multi-frequency data ranging from UV to submillimeter to trace not only the spatial but also the temporal variations of magnetic field (Yan & Lazarian 2007, 2012; Shangguan & Yan 2013; Zhang & Yan 2018).

6. SUMMARY

Polarizations of absorption lines from ground state are discovered with high polarization degree for the first time on the binary system of 89 Her. We conclude that:

- The polarization directions of the two Fe I lines show little variation across the orbital period as opposed to the polarization of many other absorption lines from the upper states in the same environment, indicating that the atoms are realigned by magnetic field on the ground state.
- The direction of polarization in the GSA regime directly points to the 2D projection of the mean magnetic field in the photosphere of the primary.

- The 90 degree (Van Vleck) degeneracy is broken from the comparison of theoretical expectation and the observed degree of polarizations.
- The polar angle between magnetic field and LOS is obtained from the analysis of the polarization degree of both Fe I lines.
- The upper limit of the mean magnetic field is $\lesssim 100\text{mG}$ in the photosphere of the primary from the fact

that the polarization from upper levels absorption lines are aligned by the radiation.

ACKNOWLEDGMENTS

We acknowledge helpful communications on various aspects of the paper with the following colleagues: F. Boulanger, S. Gao, J. Liu, R. Liu, K. Makwana, Q. Zhu. MG acknowledges the partial support from DESY during his visit there.

REFERENCES

- Akras, S., Ramírez Vélez, J. C., Nanouris, N., et al. 2017, *Mon. Not. R. Astron. Soc.*, 466, 2948, doi: [10.1093/mnras/stw3046](https://doi.org/10.1093/mnras/stw3046)
- Brossel, Jean, Kastler, Alfred, & Winter, Jacques. 1952, *J. Phys. Radium*, 13, 668, doi: [10.1051/jphysrad:019520013012066800](https://doi.org/10.1051/jphysrad:019520013012066800)
- Bujarrabal, V., van Winckel, H., Neri, R., et al. 2007, *A&A*, 468, L45, doi: [10.1051/0004-6361:20066969](https://doi.org/10.1051/0004-6361:20066969)
- Claret, A., & Bloemen, S. 2011, *A&A*, 529, A75, doi: [10.1051/0004-6361/201116451](https://doi.org/10.1051/0004-6361/201116451)
- Cohen-Tannoudji, C., Dupont-Roc, J., Haroche, S., & Laloë, F. 1969, *Physical Review Letters*, 22, 758, doi: [10.1103/PhysRevLett.22.758](https://doi.org/10.1103/PhysRevLett.22.758)
- Donati, J.-F., Catala, C., Landstreet, J. D., & Petit, P. 2006, in *Astronomical Society of the Pacific Conference Series*, Vol. 358, *Solar Polarization 4*, ed. R. Casini & B. W. Lites, 362
- Donati, J.-F., Semel, M., Carter, B. D., Rees, D. E., & Collier Cameron, A. 1997, *Mon. Not. R. Astron. Soc.*, 291, 658, doi: [10.1093/mnras/291.4.658](https://doi.org/10.1093/mnras/291.4.658)
- Gangi, M., & Leone, F. 2019, *Astronomische Nachrichten*, 340, 409, doi: [10.1002/asna.201913626](https://doi.org/10.1002/asna.201913626)
- Happer, W. 1972, *Reviews of Modern Physics*, 44, 169, doi: [10.1103/RevModPhys.44.169](https://doi.org/10.1103/RevModPhys.44.169)
- Hawkins, W. B. 1955, *Physical Review*, 98, 478, doi: [10.1103/PhysRev.98.478](https://doi.org/10.1103/PhysRev.98.478)
- Hawkins, W. B., & Dicke, R. H. 1953, *Phys. Rev.*, 91, 1008, doi: [10.1103/PhysRev.91.1008](https://doi.org/10.1103/PhysRev.91.1008)
- House, L. L. 1974, *PASP*, 86, 490, doi: [10.1086/129637](https://doi.org/10.1086/129637)
- Kastler, A. 1950, *J. Phys. Radium*, 11, 255, doi: [10.1051/jphysrad:01950001106025500](https://doi.org/10.1051/jphysrad:01950001106025500)
- Kipper, T. 2011a, *Baltic Astronomy*, 20, 65, doi: [10.1515/astro-2017-0269](https://doi.org/10.1515/astro-2017-0269)
- . 2011b, *Baltic Astronomy*, 20, 65, doi: [10.1515/astro-2017-0269](https://doi.org/10.1515/astro-2017-0269)
- Kurucz, R. L. 2005, *Memorie della Societa Astronomica Italiana Supplementi*, 8, 14
- Landi Degl’Innocenti, E. 1984, *SoPh*, 91, 1, doi: [10.1007/BF00213606](https://doi.org/10.1007/BF00213606)
- Landi Degl’Innocenti, E., & Landolfi, M., eds. 2004, *Astrophysics and Space Science Library*, Vol. 307, *Polarization in Spectral Lines*, doi: [10.1007/978-1-4020-2415-3](https://doi.org/10.1007/978-1-4020-2415-3)
- Landolfi, M., & Landi Degl’Innocenti, E. 1986, *A&A*, 167, 200
- Leone, F., Cecconi, M., Cosentino, R., et al. 2014, in *Proc. SPIE*, Vol. 9147, *Ground-based and Airborne Instrumentation for Astronomy V*, 91472F, doi: [10.1117/12.2054757](https://doi.org/10.1117/12.2054757)
- Leone, F., Avila, G., Bellassai, G., et al. 2016, *Astronomical J.*, 151, 116, doi: [10.3847/0004-6256/151/5/116](https://doi.org/10.3847/0004-6256/151/5/116)
- Leone, F., Gangi, M., Giarrusso, M., et al. 2018, *Mon. Not. R. Astron. Soc.*, 480, 1656, doi: [10.1093/mnras/sty1882](https://doi.org/10.1093/mnras/sty1882)
- Piskunov, N., Snik, F., Dolgoplov, A., et al. 2011, *The Messenger*, 143, 7
- Sabin, L., Wade, G. A., & Lèbre, A. 2015, *MNRAS*, 446, 1988, doi: [10.1093/mnras/stu2227](https://doi.org/10.1093/mnras/stu2227)
- Shangguan, J., & Yan, H. 2013, *Astrophys. J.*, 343, 335, doi: [10.1007/s10509-012-1243-y](https://doi.org/10.1007/s10509-012-1243-y)
- Strassmeier, K. G., Woche, M., Ilyin, I., et al. 2008, in *Proc. SPIE*, Vol. 7014, *Ground-based and Airborne Instrumentation for Astronomy II*, 70140N, doi: [10.1117/12.787376](https://doi.org/10.1117/12.787376)
- Van Vleck, J. H. 1925, *Proceedings of the National Academy of Science*, 11, 612, doi: [10.1073/pnas.11.10.612](https://doi.org/10.1073/pnas.11.10.612)
- Varshalovich, D. A. 1971, *Soviet Physics Uspekhi*, 13, 429, doi: [10.1070/PU1971v013n04ABEH004667](https://doi.org/10.1070/PU1971v013n04ABEH004667)
- Waters, L. B. F. M., Waelkens, C., Mayor, M., & Trams, N. R. 1993, *A&A*, 269, 242
- Yan, H., & Lazarian, A. 2006, *Astrophys. J.*, 653, 1292, doi: [10.1086/508704](https://doi.org/10.1086/508704)
- . 2007, *ApJ*, 657, 618, doi: [10.1086/510847](https://doi.org/10.1086/510847)
- . 2008, *Astrophys. J.*, 677, 1401, doi: [10.1086/533410](https://doi.org/10.1086/533410)
- . 2012, *Journal of Quantitative Spectroscopy and Radiative Transfer*, 113, 1409, doi: [10.1016/j.jqsrt.2012.03.027](https://doi.org/10.1016/j.jqsrt.2012.03.027)
- Zhang, H., & Yan, H. 2018, *Mon. Not. R. Astron. Soc.*, 475, 2415, doi: [10.1093/mnras/stx3164](https://doi.org/10.1093/mnras/stx3164)
- Zhang, H., Yan, H., & Dong, L. 2015, *Astrophys. J.*, 804, 142, doi: [10.1088/0004-637X/804/2/142](https://doi.org/10.1088/0004-637X/804/2/142)